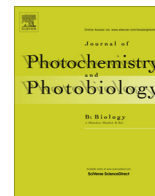




Contents lists available at ScienceDirect

Journal of Photochemistry and Photobiology B: Biology

journal homepage: www.elsevier.com/locate/jphotobiol

Synthesis, photochemistry, DNA cleavage/binding and cytotoxic properties of fluorescent quinoxaline and quinoline hydroperoxides



Nilanjana Chowdhury^a, Moumita Gangopadhyay^a, S. Karthik^a, N.D. Pradeep Singh^{a,*}, Mithu Baidya^b, S.K. Ghosh^b

^a Department of Chemistry, Indian Institute of Technology Kharagpur, Kharagpur 721302, India

^b Department of Biotechnology, Indian Institute of Technology Kharagpur, Kharagpur 721302, India

ARTICLE INFO

Article history:

Received 28 August 2013

Received in revised form 11 November 2013

Accepted 12 November 2013

Available online 22 November 2013

Keywords:

Quinoxaline

Quinoline

Hydroperoxides

Photoinduced DNA cleavage

Intercalation

Cytotoxicity

ABSTRACT

Novel fluorescent quinoxaline and quinoline hydroperoxides were shown to perform dual role as both fluorophores for cell imaging and photoinduced DNA cleaving agents. Photophysical studies of newly synthesized quinoxaline and quinoline hydroperoxides showed that they all exhibited moderate to good fluorescence. Photolysis of quinoxaline and quinoline hydroperoxides in acetonitrile using UV light above 350 nm resulted in the formation of corresponding ester compounds *via* γ -hydrogen abstraction by excited carbonyl chromophore. Single strand DNA cleavage was achieved on irradiation of newly synthesized hydroperoxides by UV light (≥ 350 nm). Both hydroxyl radicals and singlet oxygen were identified as reactive oxygen species (ROS) responsible for the DNA cleavage. Further, we showed quinoline hydroperoxide binds to ct-DNA *via* intercalative mode. In vitro biological studies revealed that quinoline hydroperoxide has good biocompatibility, cellular uptake property and cell imaging ability. Finally, we showed that quinoline hydroperoxide can permeate into cells efficiently and may cause cytotoxicity upon irradiation by UV light.

© 2013 Elsevier B.V. All rights reserved.

1. Introduction

Synthetic nucleases are of great importance for the use as structural probes and therapeutic agents [1,2]. Recently, synthetic nucleases activated by UV light (≥ 300 nm) are gaining increased interest as DNA photocleavage agents, since they can be controlled both in spatial and temporal senses [3]. Importantly, the developments of intercalating synthetic photonucleases which can recognize specific DNA sequences and result in an efficient DNA photocleavage at specific sites have become highly demanding [4,5].

Organic hydroperoxides are well known for the generation of hydroxyl radicals under photolytic condition and hence explored as efficient DNA cleaving agents. Development of organic hydroperoxides which can efficiently generate OH radicals on irradiation using UV-light above 350 nm have been well documented in the literature [6–11]. The naphthalimide hydroperoxides (Fig. 1) exhibited promising DNA cleavage capabilities under photolytic condition *via* efficient generation of hydroxyl radicals [9–11]. Further, the oxazolone naphthalimide, fluorine containing naphthalimide, and thiocyclic fused naphthalimide hydroperoxide derivatives are also reported for their efficient DNA cleaving abilities under UV light [12–15]. Even the naphthalene moiety provided organic hydroperoxides with good molar absorption above 350 nm, the

photoenhanced toxicity of naphthalene moiety remains to be a main drawback. Hence, we explored our search to other bicyclic systems which are analogous to naphthalene moiety.

Quinoxalines and quinoline derivatives have always been of great interest in medicinal chemistry because of their broad spectrum of biological activities such as antihistaminic [16], anti-trypanosomal [17], anti-herpes [18] and antiplasmodial [19]. They have also been used as Ca uptake or release inhibitor [20] and vascular smooth muscle cell proliferation inhibitor [21]. Moreover, quinoxaline moiety is a part of number of antibiotics such as echinomycin, levomycin and actinomycin which are known to inhibit the growth of gram-positive bacteria [22] and also active against various transplantable tumours [23,24]. In addition to their broad spectrum of biological activities these heterocycles have good absorption above 350 nm. More importantly these heterocycles adopt planar conformation which helps in intercalative binding with DNA. Hence, we designed a new family of organic hydroperoxides replacing naphthalene moiety by quinoxaline and quinoline system which can induce DNA cleavage on irradiation using UV light above 350 nm.

In this paper, we have discussed in detail the synthesis, characterization, photophysical and photochemical behavior of quinoxaline and quinoline hydroperoxides. Importantly, we have examined the single strand DNA cleaving ability of newly synthesized hydroperoxides by UV light (≥ 350 nm). Further, we studied the intercalative mode of binding of quinoline hydroperoxide with

* Corresponding author. Tel.: +91 3222 282324; fax: +91 3222 282252.

E-mail address: ndpradeep@chem.iitkgp.ernet.in (N.D. Pradeep Singh).

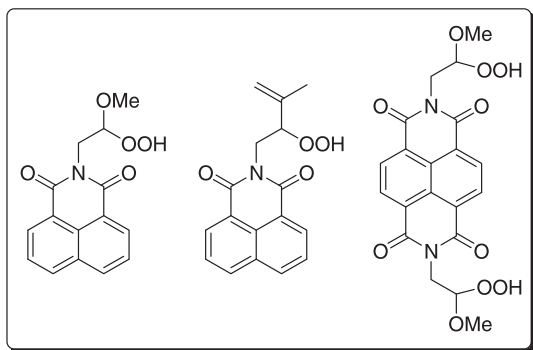


Fig. 1. Organic hydroperoxides based on naphthalene system.

ct-DNA. Finally, we investigated the toxicity of the quinoline hydroperoxide before and after irradiation against cancer cells.

2. Materials and method

2.1. General

All reactions were conducted using oven-dried glassware under an atmosphere of Argon (Ar). Commercial grade reagents were used without further purification. Solvents were dried and distilled following usual protocols. Flash chromatography was carried out using Rankem Silica gel (230–400 mesh) purchased from Rankem, India. TLC was performed on aluminium-backed plates coated with Silica gel 60 with F₂₅₄ indicator (Merck). The ¹H NMR spectra were measured with Bruker-200 (200 MHz), Bruker-400 (400 MHz) and ¹³C NMR spectra were measured with Bruker-200 (50 MHz), Bruker-400 (100 MHz) using CDCl₃ and d₆-DMSO. ¹H NMR chemical shifts are expressed in parts per million (δ) downfield to CDCl₃ (δ = 7.26) and d₆-DMSO (δ = 2.54). ¹³C NMR chemical shifts are expressed in parts per million (δ) relative to the central CDCl₃ resonance (δ = 77.0) and central d₆-DMSO resonance (δ = 40.45). Coupling constants in ¹H NMR are expressed in Hz. Mass spectra were analyzed by Waters LCT mass spectrometer. Elemental analysis was carried out with ParkinElmer 2400-II. UV/vis absorption spectra were recorded on a Shimadzu UV-2450 UV/vis spectrophotometer. Melting points were measured in Toshniwal (India) melting point apparatus. pBR 322 DNA was used. Photolysis was carried out using 125 W medium pressure mercury lamp supplied by SAIC (India). DNA binding experiments were conducted in sodium phosphate buffer (10 mM, pH 7.0 containing 50 mM NaCl) using ethanolic solution of quinoline hydroperoxide **10b**. The solution of quinoline hydroperoxide was prepared in absolute ethanol due to their relative insolubility in pure aqueous medium and their dilute solutions in buffer were used for experiments. Double distilled water was used for solution preparation. Calf thymus DNA (ca. 350 mM NP) in this buffer medium gave a ratio of ca. 1.9: 1 of UV absorbance at 260 and 280 nm indicating that the DNA is apparently free from protein. The concentration of DNA was estimated from its absorption intensity at 260 nm with a known molar extinction coefficient value (ϵ) of 6600 dm³ mol⁻¹ cm⁻¹ [25]. The concentrations were determined spectrophotometrically by using the molar extinction coefficient (ϵ) at 476 nm = 5680 M⁻¹ cm⁻¹ for ethidium bromide in distilled water [26].

2.2. General procedure for the synthesis of quinoxaline hydroperoxides **5a–b**

2.2.1. Synthesis of compounds **3a–b**

2.2.1.1. Preparation of 3-Phenyl-1H-quinoxalin-2-one (**3a**). *o*-Phenylene diamine **1** (1 g, 9.25 mmol) and ethyl 2-oxo-2-phenylacetate **2a** (2.47 g

13.8 mmol) in methanol was refluxed for 30 min at 78 °C. White solids were started forming during the course of the reaction under refluxing condition. After completion of the reaction the solid precipitate was filtered to get compound **3a** in good yield (1.28 g, 80%). Similar procedure was followed for the synthesis of compounds **3b**.

2.2.2. Synthesis of compounds **4a–b**

2.2.2.1. Preparation of 1-(2,2-Dimethoxy-ethyl)-3-phenyl-1H-quinoxalin-2-one (**4a**). To a solution of compound **3a** (0.36 g, 1.62 mmol) in dry DMF, Cs₂CO₃ (1 g, 3.07 mmol) was added. Then, neat 2-bromo-1,1-dimethoxyethane (0.23 mL, 1.94 mmol) was added to the reaction mixture and heated to 80 °C and stirred the reaction mixture for 4 h. After completion of the reaction, the reaction mixture was diluted with EtOAc and washed with water for 2–3 times. Evaporation of the organic phase gave an oily residue, which was purified by column chromatography using as eluent a mixture of 40% EtOAc/hexane to obtain compound **4a** (0.281 g, 70%) as white solid in moderate yield. Similar procedure was followed for the synthesis of compound **4b**.

2.2.3. Synthesis of quinoxaline hydroperoxides **5a–b**

2.2.3.1. Preparation of 1-(2-hydroperoxy-2-methoxy-ethyl)-3-phenyl-1H-quinoxalin-2-one (**5a**). To a solution of compound **4a** (310 mg, 1 mmol) in dry DCM, ethereal H₂O₂ (50%) solution was added under ice cooled condition. The catalytic amount of triflic acid (2 drops, 20 mol%) in dry DCM was added to the reaction mixture under same condition. The reaction was stirred at 35 °C for 5–6 h. After completion of the reaction, the reaction mixture was diluted with DCM and washed with water. Evaporation of the organic phase gave an oily residue, which was purified by column chromatography using as eluent a mixture of 35% EtOAc/hexane to obtain compound **5a** (0.20 g, 65%) as white solid in moderate yield. Similar procedure was followed for the synthesis of compound **5b**.

2.3. General procedure for synthesis of quinoline hydroperoxides **10a–b**

2.3.1. Synthesis of compound **8a–b**

2.3.1.1. Preparation of 1H-quinolin-2-one (**8a**). Compound **7a** (1.3 g, 6.19 mmol) and anhydrous AlCl₃ (2.47 g, 18.6 mmol) was mixed together and heated at 100 °C unless it melted properly. Then, the reaction mixture was cooled to room temperature. Ice water was added to the solution and the resulting precipitates were collected, washed with water and 5% HCl to give the desired product **8a** (0.7 g, 80%) in good yield. Compound **8b** was also prepared by using similar procedure.

2.3.2. Synthesis of compound **9a–b**

2.3.2.1. Preparation of 1-(2,2-dimethoxy-ethyl)-1H-quinolin-2-one (**9a**). To a solution of compound **8a** (0.3 g, 2.07 mmol) in dry DMF, Cs₂CO₃ (0.963 g, 2.5 mmol) was added. Then, neat 2-bromo-1,1-dimethoxyethane (0.28 mL, 2.48 mmol) was added to the reaction mixture and heated to 50 °C and stirred the reaction mixture for 4 h. After completion of the reaction, the reaction mixture was diluted with EtOAc and washed with water. Evaporation of the organic phase gave an oily residue, which was purified by column chromatography using as eluent a mixture of 30% EtOAc/hexane to afford compound **9a** (0.35 g, 72%) in good yield. Compound **9b** was also prepared by using similar procedure.

2.3.3. Synthesis of quinoline hydroperoxides **10a–b**

2.3.3.1. 1-(2-Hydroperoxy-2-methoxy-ethyl)-1H-quinolin-2-one (**10a**). To a solution of compound **9a** (300 mg, 1.29 mmol) in dry DCM, ethereal H₂O₂ (50%) solution was added under ice cooled condition. Then catalytic amount of triflic acid (2 drops, 20 mol%) in dry DCM was added to the reaction mixture under

ice cooled condition. The reaction was stirred at 35 °C for 4–5 h. After completion of the reaction, the reaction mixture was diluted with DCM and washed with water. Evaporation of the organic phase gave an oily residue, which was purified by column chromatography using as eluent a mixture of 25% EtOAc/hexane to afford compound **10a** in moderate yield (0.16 g, 56%). Compound **10b** was also prepared by using similar procedure.

2.4. Preparative photolysis of quinoxaline and quinoline hydroperoxides **5b** and **10b**

Photolysis of quinoxaline and quinoline hydroperoxides **5b** and **10b** (200 mg, 0.7 mM) in 80 mL argon saturated acetonitrile solution were carried out using 125 W medium pressure Hg lamp as light source (≥ 350 nm) and 0.1 M CuSO₄ solution as UV cut-off filter. The reactions were monitored by TLC at regular interval of time. After completion of photolysis, solvent was removed under reduced pressure and photoproducts were isolated by flash column chromatography using 20%EtOAc/hexane as an eluent. The ester compounds **11** and **12** were isolated as major photoproducts along with minor amounts of **3b** and **8b**.

2.5. DNA cleavage experiments

2.5.1. Procedure for DNA cleaving ability of quinoline hydroperoxide **10b** at different concentrations

The reaction mixtures (20 μ L) containing supercoiled circular pBR322 DNA stock solution (form I, 62.5 μ g/mL) in sodium phosphate buffer (10 mM, pH 7.0), quinoline hydroperoxide **10b** at different concentrations (10–50 μ M) in 10% acetonitrile solution individually in a eppendorf were irradiated with UV light (≥ 350 nm) under aerobic conditions at room temperature for 10 min. The sample buffer containing bromophenol and glycerol was added to the reaction mixture and loaded on 1% agarose gel. After addition of the tank buffer (1X TAE), the electrophoresis apparatus was attached to a power supply. The gel was visualized by GEL LOGIC 200 Imaging System.

2.5.2. General procedure for photoinduced DNA cleavage by quinoxaline and quinoline **5a–b** and **10a–b**

The DNA cleavage experiments were carried out containing pBR322 DNA stock solution in sodium phosphate buffer (10 mM, pH 7.0), hydroperoxides **5a–b** and **10a–b** (30 μ M) in 10% acetonitrile solution individually in a eppendorf upon irradiation of UV light (≥ 350 nm) for 10 min. The sample buffer containing bromophenol and glycerol was added to the reaction mixture and loaded on 1% agarose gel. After addition of the tank buffer (1X TAE), the electrophoresis apparatus was attached to a power supply. The gel was visualized by GEL LOGIC 200 Imaging System.

2.5.3. Photoinduced DNA cleavage of quinoline hydroperoxide **10b** in different concentration of NaN₃

The photoinduced DNA cleavage experiments were carried out in presence of increasing amount of NaN₃ in the sodium phosphate buffer solution containing quinoline hydroperoxide **10b** (30 μ M) in 10% acetonitrile solution, upon irradiation of UV light (≥ 350 nm,) under aerobic condition at room temperature for 10 min. The sample buffer containing bromophenol and glycerol was added to the reaction mixture and loaded on 1% agarose gel. After addition of the tank buffer (1X TAE), the electrophoresis apparatus was attached to a power supply. The gel was visualized by GEL LOGIC 200 Imaging System.

2.5.4. Photoinduced DNA cleavage of quinoline hydroperoxide **10b** by adding different additives

The photoinduced DNA cleavage experiments were done by adding different additives like D₂O (4 μ L), DMSO (4 μ L), KI (50 mM) in sodium phosphate buffer solution containing quinoline hydroperoxide **10b** (30 μ M) in 10% acetonitrile solution, upon irradiation of UV light (≥ 350 nm) under aerobic condition at room temperature for 10 min. The sample buffer containing bromophenol and glycerol was added to the reaction mixture and loaded on 1% agarose gel. After addition of the tank buffer (1X TAE), the electrophoresis apparatus was attached to a power supply. The gel was visualized by GEL LOGIC 200 Imaging System.

2.6. DNA-binding studies of quinoline hydroperoxide **10b**

2.6.1. Electronic absorption titration of quinoline hydroperoxide **10b**

Absorption titration experiments were performed in 3 cm quartz cuvette by taking absorption in between 300 and 400 nm. 3 mL of 50 μ M quinoline hydroperoxide **10b** in ethanolic solution was titrated with increasing concentration of ct-DNA (0–100 μ M) in phosphate buffer (10 mM, pH 7.0) containing 50 mM NaCl

2.6.2. Fluorimetric titration of quinoline hydroperoxide **10b**

Fluorimetric titrations were performed in a 3 cm quartz cuvette using an excitation wavelength of 350 nm having emission maxima at 400 nm. The titration experiments were performed with fixed concentrations of quinoline hydroperoxide **10b** (50 μ M) in ethanolic solution, with gradually increasing the concentration of ct-DNA (0–100 μ M) in phosphate buffer (10 mM, pH 7.0) containing 50 mM NaCl. A quantitative estimation of quenching experiments in term of the binding constant calculation is obtained from Stern–Volmer equation

$$\log(F_0 - F)/F = \log K_b + n \log[\text{DNA}] \quad (1)$$

where K_b and n are the binding constant and the number of binding sites respectively, [DNA] is the concentration of ct-DNA in base pairs, F_0 and F are the fluorescence intensities of quinoline hydroperoxide **10b** in absence and presence of DNA respectively. From the linear plot of $\log(F_0 - F)/F$ vs \log DNA, the binding constant (K_b) value was calculated.

2.6.3. Ethidium bromide (EB) displacement assay of quinoline hydroperoxide **10b**

Fluorimetric titrations were performed in a 3 cm quartz cuvette using an excitation wavelength of 480 nm. 3 mL of 20 μ M ct-DNA was saturated with 2 μ M of ethidium bromide (EB) solution in 10 mM phosphate buffer pH 7.0 containing 50 mM NaCl. The EB-ct-DNA solution was then titrated by successive addition of hydroperoxide **10b** to reach a final concentration of ~ 35 μ M. Emission spectra were recorded from 500 nm to 750 nm. The spectra were analyzed according to the classical Stern–Volmer equation

$$F_0/F = 1 + K_{sv}[Q] \quad (2)$$

where F_0 and F are the fluorescence intensities of ethidium bromide in absence and presence of hydroperoxide **10b** respectively, K_{sv} is the linear Stern–Volmer quenching constant, [Q] is the concentration of the hydroperoxide **10b**.

2.7. Docking studies of quinoline hydroperoxide **10b**

The B-DNA crystal structure used for the docking studies was obtained from the Protein Data Bank (PDB ID: 453D) [27]. The DNA file was prepared for docking by removing water molecules and adding polar hydrogen atoms with Gasteiger charges. The 3D structure of the ligands was generated in Sybyl 6.92 (Tripos Inc., St. Louis, USA) and its energy-minimized conformation was

obtained with the help of the MMFF94 force field using MMFF94 charges. The rotatable bonds in the ligand were assigned with AutoDockTools and docking was carried out with AutoDock 4.0 Lamarckian Genetic Algorithm (GA) [28]. DNA was enclosed in a grid having 0.375–0.431 Å spacing. Other miscellaneous parameters were assigned the default values given by AutoDock. The output from AutoDock was rendered in PyMol [29].

2.8. Confocal microscopy of hydroperoxide **10b**

HeLa cells grown overnight in a 24-well plate, were treated with various concentrations of quinoline hydroperoxide **10b** (4, 10, 20 μM) for 1 h. Media was then aspirated and was thoroughly washed with phosphate buffered saline (PBS) and was analyzed with confocal microscope (FV1000, Olympus) for detection of cellular uptake of the hydroperoxide **10b**.

2.9. Cell cytotoxicity assay of hydroperoxide **10b**

The photocytotoxicity of quinoline hydroperoxide **10b** was studied using MTT assay which is based on the ability of mitochondrial dehydrogenases of viable cells to cleave the tetrazolium rings of MTT forming dark purple membrane impermeable crystals of formazan that can be quantified at 540 nm after solubilization in DMSO. Cytotoxicity of quinoline hydroperoxide **10b** was determined with and without irradiation of UV light on human cervical HeLa cancer cells. Cells in their exponential growth phase were trypsinized and seeded in 96-well flat-bottom culture plates at a density of 10^4 cells per well in 100 μL complete Dulbecco's Modified Eagle's Medium (DMEM). The cells were allowed to adhere and grow for 24 h at 37 °C in an incubator in presence of 5% CO_2 and then the medium was replaced with 100 μL fresh incomplete DMEM medium containing different concentrations of hydroperoxide **10b** (0–100 μM). Cells were then incubated for 12 h, after which the culture medium was replaced with fresh phosphate buffered saline (PBS). Chemically treated cells were irradiated with UV light for 30 min and further incubated for about 48 h at 37 °C. Medium was aspirated and 100 μL of 1 mg/mL MTT reagent in PBS was added to each well and incubated for 4 h; during this period active mitochondria of viable cells reduce MTT to purple formazan. Unreduced MTT were discarded and the formazan precipitate was dissolved in DMSO (100 μL). Optical Density (OD) was measured spectrophotometrically using a microplate reader (Biorad, USA) at 570 nm. The cytotoxic effect of each treatment was expressed as percentage of cell viability relative to the untreated control cells. The IC_{50} values were calculated using Prism nonlinear regression analysis using GraphPad Prism 5 software.

3. Result and discussion

3.1. Synthesis of quinoxaline and quinoline hydroperoxides

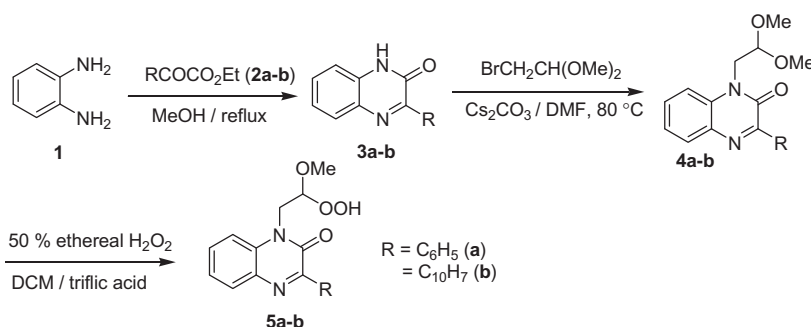
We have synthesized quinoxaline hydroperoxides **5a–b** as illustrated in Scheme 1. α -Ketoesters **2a–b** were synthesized following the literature procedure [30]. Condensation reaction of *o*-phenylenediamine (**1**) with α -ketoesters in methanol under refluxing condition resulted in quinoxalines **3a–b** in excellent yields [31]. Then **4a–b** were synthesized by alkylation of **3a–b** with 2-bromo-1,1-dimethoxy ethane [$\text{BrCH}_2\text{CH}(\text{OMe})_2$] in presence of 1.5 equivalent cesium carbonate (Cs_2CO_3) in DMF at 80 °C under inert condition. Quinoxaline hydroperoxides **5a–b** were prepared by treating **4a–b** with 50% ethereal H_2O_2 in DCM in presence of 20 mol% triflic acid at room temperature under inert condition [32].

Quinoline hydroperoxides **10a–b** were also synthesized as shown in Scheme 2. First condensation reactions were carried out between arylamines **6a–b** and cinnamyl chloride to obtain the unsaturated amides **7a–b** in excellent yields [33]. Intramolecular Fridel-Crafts reaction of amides **7a–b** in presence of 3 equivalents anhydrous AlCl_3 afforded quinolines **8a–b** respectively [34]. Then quinolines **9a–b** were synthesized from **8a–b** by alkylation with $\text{BrCH}_2\text{CH}(\text{OMe})_2$. Quinoline hydroperoxides **10a–b** were synthesized by treating **9a–b** with 50% ethereal H_2O_2 in DCM in presence of 20 mol% triflic acid at room temperature under inert condition as shown in Scheme 2. Quinoxaline and quinoline hydroperoxides **5a–b** and **10a–b** were characterized by NMR, mass spectroscopy and elemental analysis. The hydroperoxide compounds **5a–b** and **10a–b** were stable at 0° C in the dark up to 3 months.

3.2. Photophysical properties of quinoxaline and quinoline hydroperoxides

The UV/vis absorption and emission spectra of degassed 1×10^{-5} M solution of quinoxaline and quinoline hydroperoxides **5a–b** and **10a–b** was recorded in absolute ethanol. The absorption spectra of quinoxaline hydroperoxides **5a–b** showed absorption maxima at 360 nm ($\log \epsilon = 3.3 \text{ mol}^{-1} \text{ L cm}^{-1}$) (Fig. 2a), whereas the emission maxima were found to be red shifted to about 441–450 nm (Table 1). On the other hand, quinoline hydroperoxides **10a** and **10b** showed an absorption maxima at 330 ($\log \epsilon = 3.21 \text{ mol}^{-1} \text{ L cm}^{-1}$) and 370 ($\log \epsilon = 3.4 \text{ mol}^{-1} \text{ L cm}^{-1}$) nm (Fig. 2b), whereas the emission maxima were found to be at 390 nm and 417 nm respectively (Table 1).

The Stokes' shift was calculated from the difference in the absorption and the emission maxima and the magnitude of the Stokes' shift of quinoxaline hydroperoxides **5a–b** varied between 81–90 nm, whereas for **10a–b**, it varied from 47–60 nm. Further, hydroperoxides **5a–b** and **10a–b** showed low to moderate fluores-



Scheme 1. Synthesis of quinoxaline hydroperoxides **5a–b**.

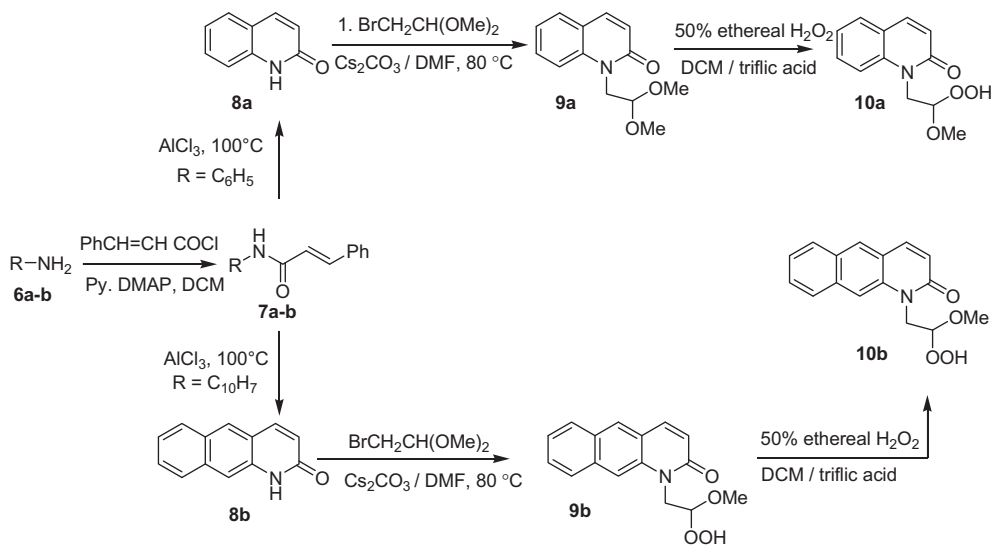
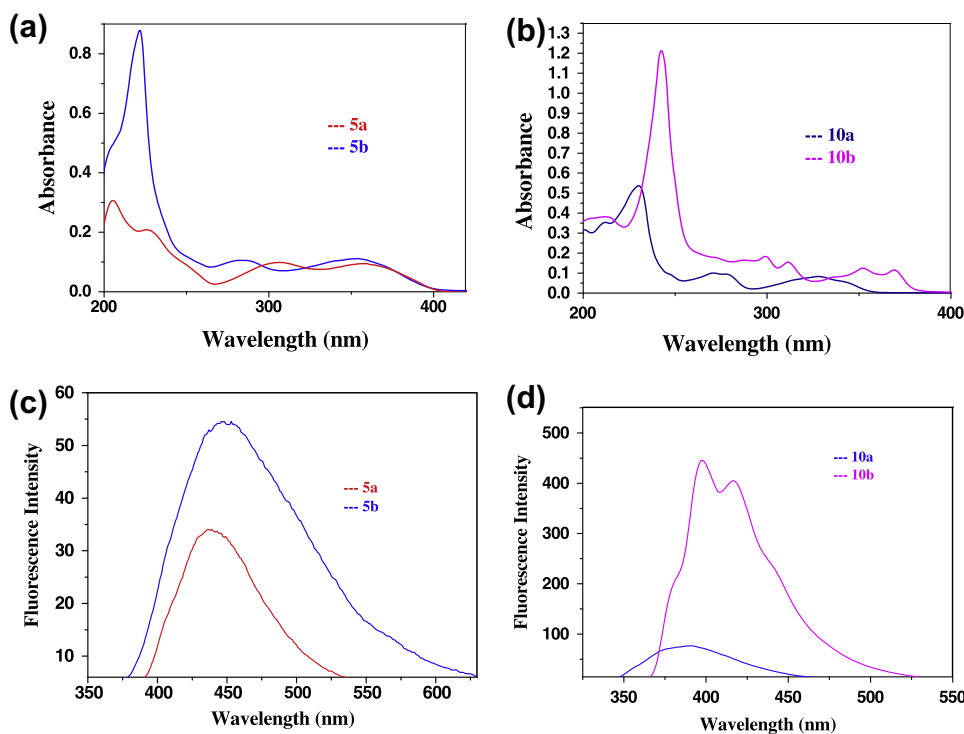
Scheme 2. Synthesis of quinoline hydroperoxides **10a–b**.

Fig. 2. (a) UV/vis absorption spectra of quinoxaline hydroperoxides **5a–b** in ethanol (1×10^{-5} M). (b) UV/vis absorption spectra of quinoline hydroperoxides **10a–b** in ethanol (1×10^{-5} M). (c) Fluorescence spectra of quinoxaline hydroperoxides **5a–b** in ethanol (1×10^{-5} M). (d) Fluorescence spectra of quinoline hydroperoxides **10a–b** in ethanol (1×10^{-5} M).

cence quantum yield ($0.005 < \Phi < 0.020$). The absorption and emission maxima (λ_{\max}), molar absorptivities (ϵ) and fluorescence quantum yields (Φ_F) of above hydroperoxides are summarized in Table 1. Fluorescence quantum yields were calculated using anthracene as standard ($\Phi_F = 0.27$ in ethanol) [35].

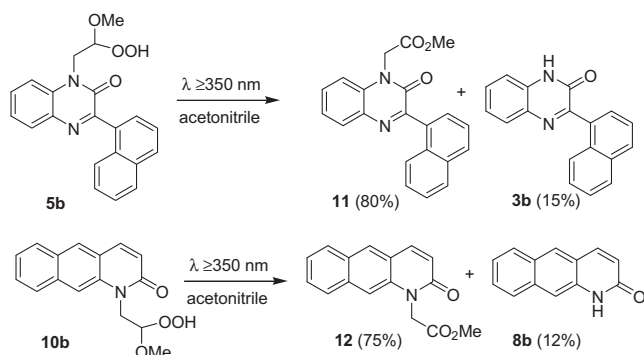
3.3. Photochemical study of quinoxaline and quinoline hydroperoxides

To understand the photochemical behavior of newly synthesized quinoxaline and quinoline hydroperoxides, we carried out the photolysis of quinoxaline and quinoline hydroperoxides **5b**

and **10b** (0.3 mM) individually, in an argon saturated acetonitrile solution using 125 W medium pressure Hg lamp as UV light source (≥ 350 nm) and 0.1 M CuSO_4 solution as UV cut-off filter. The photolysis was continued for 30 min and the course of the photolysis was monitored by TLC. After completion of the reaction, the photoproducts were isolated using flash column chromatography and characterized by NMR and mass spectroscopy. We found that quinoxaline and quinoline hydroperoxides **5b** and **10b** produced the corresponding ester compounds **11** and **12** respectively as major photoproducts [5]. Minor amount of quinoxaline **3b** and quinoline **8b** were also generated during the

Table 1
Synthetic yields, UV/vis and fluorescence data of quinoxaline and quinoline hydroperoxides **5a–b** and **10a–b**.

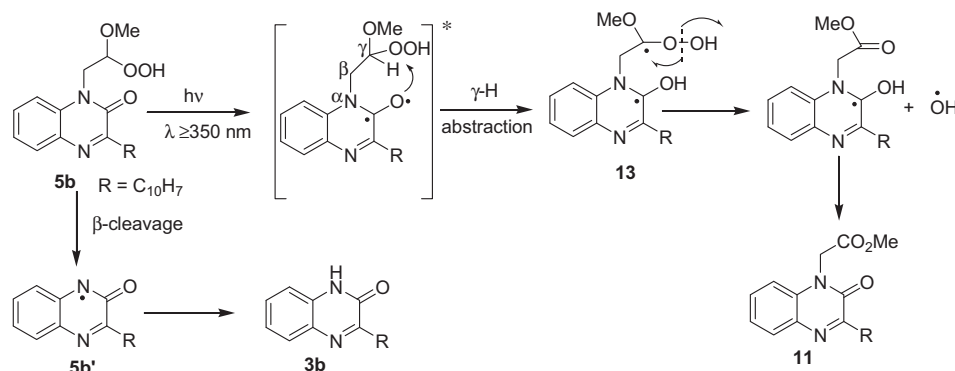
Entry	Hydroperoxides	Synthetic yield (%) ^a	UV/vis		Fluorescence		
			λ_{\max} (nm) ^b	$\log \epsilon^c$	λ_{\max} (nm) ^d	Stokes' shift (nm) ^e	$(\phi_F)^f$
1	5a	75	360	3.32	441	81	0.005
2	5b	70	360	3.38	450	90	0.007
3	10a	82	330	3.21	390	60	0.008
4	10b	60	370	3.41	417	47	0.020

^a Based on isolated yield.^b Maximum absorption wavelength.^c Molar absorption coefficient (in mol⁻¹ L cm⁻¹) at the maximum absorption wavelength.^d Maximum emission wavelength.^e Difference between maximum absorption wavelength and maximum emission wavelength.^f Fluorescence quantum yield (error limit within $\pm 5\%$).**Scheme 3.** Photolysis of quinoxaline (**5b**) and quinoline (**10b**) hydroperoxides in acetonitrile.

course of photolysis of hydroperoxides **5b** and **10b** respectively (Scheme 3).

3.3.1. Mechanism for the photolysis of hydroperoxides

Photolysis of **5b** in acetonitrile ($\lambda \geq 350$ nm) proceeded rapidly to give ester compound **11** as major product. The formation of the ester product **11** can be explained based on the well known photochemical γ -hydrogen abstraction by carbonyl chromophore of quinoxaline hydroperoxide **5b**. The latter produced hydroperoxyalkyl radical **13**, which underwent facile β -cleavage of the labile O–O bond to produce the ester product **11**. The formation of minor product **3b** can be explained by the β -carbonyl cleavage of compound **5b**. The latter gave radical **5b'**, which underwent hydrogen abstraction from the solvent (Scheme 4). Similar mechanism can also be postulated for quinoline hydroperoxides.

**Scheme 4.** Possible mechanism for the photolysis of quinoxaline hydroperoxide **5b**.

3.4. Photoinduced DNA cleaving ability of quinoxaline and quinoline hydroperoxides

To assess the DNA cleaving ability of quinoxaline and quinoline hydroperoxides, initially we carried out irradiation of supercoiled circular pBR322 plasmid DNA at room temperature under aerobic condition for a period of 10 min at different concentrations of quinoline hydroperoxide **10b** (10–50 μ M) in 10% acetonitrile and sodium phosphate buffer (pH 7.0, 10 mM) using UV light (≥ 350 nm). The results from gel electrophoresis on 1.0% agarose gel with ethidium bromide staining indicated that **10b** caused the single strand cleavage of DNA (form I) to give the relaxed circular DNA (form II). We also noticed that DNA cleaving ability of **10b** was also dependent on its concentration (Fig. 3).

Based on the above concentration study, the photoinduced DNA cleaving ability of quinoxaline and quinoline hydroperoxides **5a–b** and **10a–b** were investigated using 30 μ M concentration by irradiating using UV light (≥ 350 nm) for 10 min. The gel electrophoresis results were presented in a bar diagram which showed that all the hydroperoxides exhibited almost moderate to good DNA cleaving efficiency (Fig. 4).

To identify the reactive oxygen species responsible for photoinduced DNA cleavage by hydroperoxides, quinoline hydroperoxide **10b** was studied under different conditions.

First, to understand the role of singlet oxygen in DNA cleavage process, control experiments were carried out using NaN₃, a known singlet oxygen quencher [36,37]. The experiments were carried out by adding increasing amounts of NaN₃ in the phosphate buffer solution containing quinoline hydroperoxide **10b** at a concentration of 30 μ M along with supercoiled circular pBR322 DNA. The generated form II DNA was found to be decreased from 82% to 62% with increasing amount of NaN₃ from 5 to 100 mM (Fig. 5).

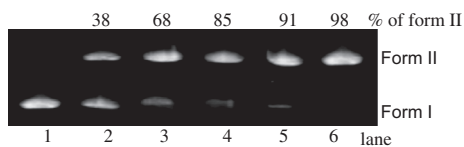


Fig. 3. Single strand cleavage of supercoiled circular pBR322 DNA (form I) to relaxed circular DNA (form II) was carried out by quinoline hydroperoxide **10b** at different concentrations (10–50 μM) upon irradiation of UV light (≥ 350 nm) for 10 min. lane 1, DNA alone; lane 2, DNA + **10b** (10 μM); lane 3, DNA + **10b** (20 μM); lane 4, DNA + **10b** (30 μM); lane 5, DNA + **10b** (40 μM); lane 6, DNA + **10b** (50 μM).

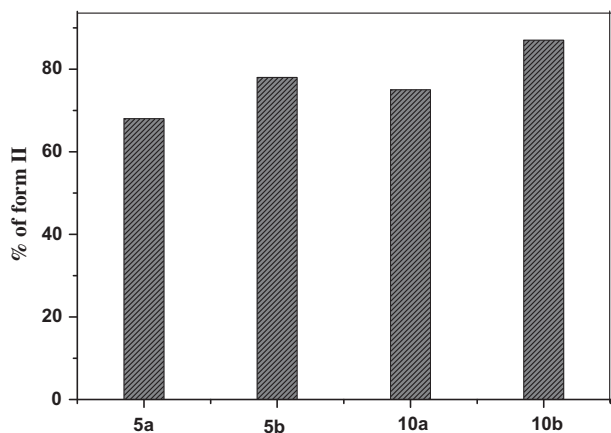


Fig. 4. Bar diagram displaying the single strand cleavage of supercoiled circular pBR322 DNA (form I) to relaxed circular DNA (form II) by quinoxaline and quinoline hydroperoxides **5a–b** and **10a–b** (30 μM) upon irradiation of UV light (≥ 350 nm) in sodium phosphate buffer (pH 7.0, 10 mM) under aerobic condition at room temperature for 10 min. The resultant products were subjected to electrophoresis on 1% agarose gel followed by ethidium bromide staining under UV light.

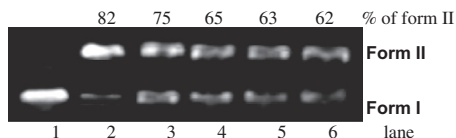


Fig. 5. Single strand cleavage of supercoiled circular pBR322 DNA (form I) to relaxed circular DNA (form II) was carried out by quinoline hydroperoxide **10b** (30 μM) in presence of increasing amount of NaN_3 (5–200 mM) in sodium phosphate buffer (pH 7.0, 10 mM) upon irradiation of UV light (≥ 350 nm) under aerobic condition at room temperature for 10 min. The resultant products were subjected to electrophoresis on 1% agarose gel followed by ethidium bromide staining under UV light. lane 1, DNA alone; lane 2, DNA + **10b** + NaN_3 (5 mM); lane 3, DNA + **10b** + NaN_3 (20 mM); lane 4, DNA + **10b** + NaN_3 (50 mM); lane 5, DNA + **10b** + NaN_3 (100 mM); lane 6, DNA + **10b** + NaN_3 (200 mM).

Further increase in the amount of NaN_3 from 100 to 200 mM has no effect on the percentage of form II DNA. Thus the contribution resulting from singlet oxygen to DNA cleavage is $\approx 38\%$.

Further, to confirm the role of singlet oxygen in DNA cleavage process, the photoinduced DNA cleavage experiments of quinoline hydroperoxide **10b** (30 μM) were carried out in O_2 saturated solution as well as in presence of D_2O .

In O_2 saturated solution we observed slight increase in DNA cleaving ability of **10b** in comparison to aerobic condition. The DNA cleavage efficiency of **10b** was further increased in presence of D_2O which can be attributed due to the longer lifetime of $^1\text{O}_2$ in D_2O medium (Fig. 6). [38]. The above results suggested that singlet oxygen is playing an important role in the DNA cleavage process.

Secondly, to prove the involvement of hydroxyl radical in the DNA cleavage mechanism, the DNA cleavage experiments were

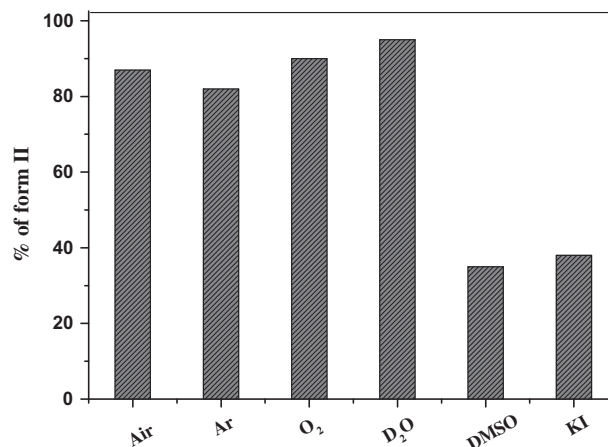


Fig. 6. Bar diagram displaying the single strand cleavage of supercoiled circular pBR322 DNA (form I) to relaxed circular DNA (form II) by quinoline hydroperoxide **10b** (30 μM) in presence of various additives in sodium phosphate buffer (pH 7.0, 10 mM) upon irradiation of UV light (≥ 350 nm) under aerobic condition at room temperature for 10 min. The resultant products were subjected to electrophoresis on 1% agarose gel followed by ethidium bromide staining under UV light. The additive concentrations/quantities are: D_2O (4 μL); DMSO (4 μL); KI (50 mM).

carried out in presence of hydroxyl radical scavengers, viz. DMSO (4 μL) and KI (50 mM) individually, along with the 30 μM concentration of quinoline hydroperoxide **10b** on irradiation using UV light ≥ 350 nm. From Fig. 6, it was clear that form II DNA was not generated significantly in presence of DMSO and KI which suggested that DNA cleavage was inhibited significantly [39,40]. The inhibition of the DNA cleavage activity in presence of DMSO and KI concluded that hydroxyl radical as a reactive oxygen species (ROS) was responsible for the photocleavage of DNA. Finally, to demonstrate the hydroxyl radical is generated by quinoline hydroperoxide or molecular oxygen we carried out DNA cleavage experiment of **10b** under argon saturated solution. The DNA cleavage ability of **10b** was found to be almost similar to aerobic condition which suggested that hydroperoxides are source for hydroxyl radical (Fig. 6).

From the above control experiments it was concluded that both singlet oxygen as well as hydroxyl radicals perform important role in DNA cleavage process.

3.5. DNA-binding studies of quinoline hydroperoxide **10b**

The DNA cleavage experiment showed that among quinoxaline and quinoline hydroperoxides, quinoline hydroperoxide **10b**

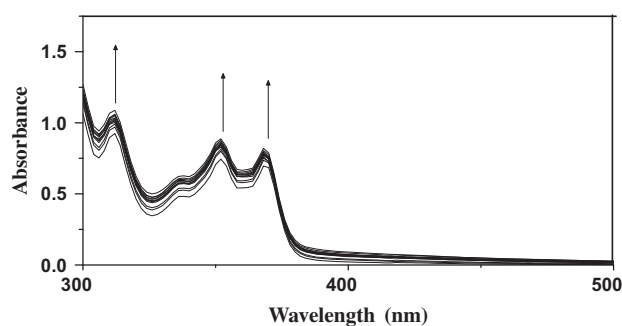


Fig. 7. Change in UV/vis absorption spectra of quinoline hydroperoxide **10b** (50 μM) in absence (bottom) and presence of ct-DNA in sodium phosphate buffer (10 mM, pH 7.0) containing 50 mM NaCl. Arrow shows that the absorbance changes upon increasing ct-DNA concentration. DNA concentrations were varied from bottom to top (0–100 μM) with increments of 5 μM of ct-DNA.

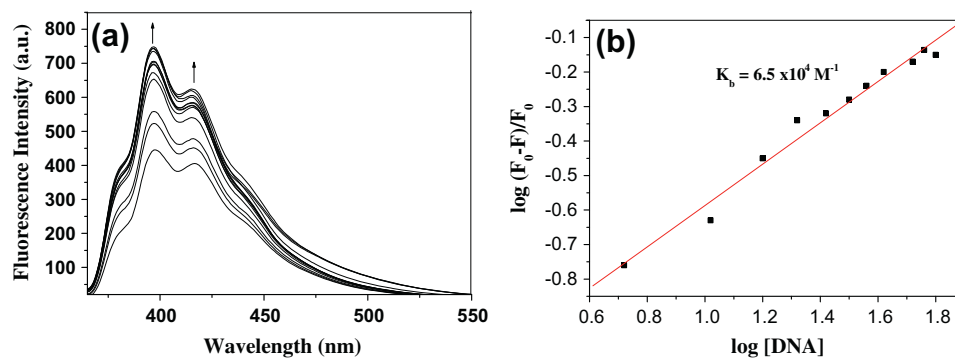


Fig. 8. (a) Fluorescence emission spectra of quinoline hydroperoxide **10b** (50 μM) in phosphate buffer (10 mM, pH 7.0) containing 50 mM NaCl with increasing concentration of ct-DNA. Arrow shows that the fluorescence changes upon increasing ct-DNA concentration. The DNA concentrations were varied from bottom to top (0–100 μM) with increments of 5 μM concentration of ct-DNA. Excitation wavelength (λ_{ex}) = 350 nm; Emission wavelength (λ_{em}) = 400 nm; (b) Plot of $\log(F_0 - F)/F_0$ vs $\log[\text{DNA}]$.

showed efficient DNA cleaving ability. Hence, we carried out DNA binding experiments, cell imaging and cytotoxicity studies in cancerous cells using quinoline hydroperoxide **10b**.

3.5.1. Electronic absorption spectroscopy

The electronic absorption spectroscopy is normally used to understand the binding properties of organic ligand with ct-DNA. The absorption spectrum of quinoline hydroperoxide **10b** was recorded in absence and presence of ct-DNA. Fig. 7 showed that upon increasing concentration of ct-DNA in the solution of **10b**, the absorption bands at 312, 350 and 370 nm showed hyperchromism shift. The hyperchromic effect in the absorption spectra suggested the interaction between the ct-DNA and hydroperoxide compound **10b** via intercalative mode of binding [41,42].

Fig. 7 Change in UV/vis absorption spectra of quinoline hydroperoxide **10b** (50 μM) in absence (bottom) and presence of ct-DNA in sodium phosphate buffer (10 mM, pH 7.0) containing 50 mM NaCl. Arrow shows that the absorbance changes upon increasing ct-DNA concentration. DNA concentrations were varied from bottom to top (0–100 μM) with increments of 5 μM of ct-DNA

3.5.2. Fluorescence spectroscopy

As quinoline hydroperoxide **10b** exhibited good fluorescence, the binding characteristics between ct-DNA and quinoline hydroperoxide **10b** were studied using fluorescence spectroscopy. The fluorescence emission spectra of **10b** in absence and presence of ct-DNA was shown in Fig. 8a. Quinoline hydroperoxide **10b** has

emission maximum at 400 nm on excitation at 350 nm (absorption maximum). Fig. 8a showed a regular increase in the fluorescence intensity of **10b** with increase of DNA concentration without any shift in the fluorescence emission maximum which indicated the intercalative mode of binding interaction of ct-DNA with **10b** [43].

The binding constant K_b was determined from the plot of $\log(F_0 - F)/F_0$ vs $\log[\text{DNA}]$ and was found to be $6.5 \times 10^4 \text{ M}^{-1}$ (Fig. 8b).

3.5.3. Ethidium bromide displacement study

To substantiate the intercalative mode of binding between quinoline hydroperoxide **10b** and ct-DNA, ethidium bromide displacement study was carried out. Ethidium bromide (EB) is one of the most sensitive fluorescence probes having a planar structure that binds DNA by an intercalative mode [44].

The fluorescence of ethidium bromide (EB) increases after DNA intercalation. Upon intercalation into DNA helix by quinoline hydroperoxide **10b**, it leads to a decrease in the binding sites of DNA available for EB, which in turn decreases the fluorescence intensity of the EB–DNA system. Fig. 9a showed the fluorescence emission spectrum of EB with and without ct-DNA and the effect of the addition of **10b** to EB bound ct-DNA. The fluorescence intensity of the EB complexed ct-DNA was decreased with increasing concentration of quinoline hydroperoxide **10b**. The quenching of EB bound to ct-DNA by **10b** was calculated in terms of Stern–Volmer quenching constant from the Stern–Volmer equation [45]. The K_{sv} value for quinoline hydroperoxide **10b** was found to be $8.92 \times 10^3 \text{ M}^{-1}$ (Fig. 9b) which suggest that quinoline

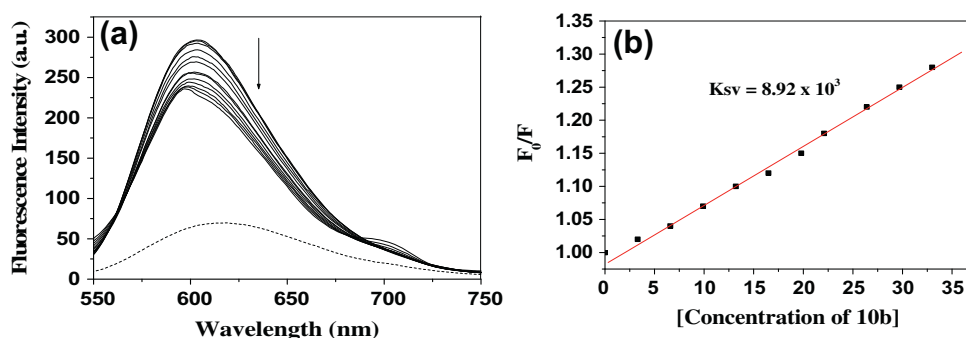


Fig. 9. (a) Fluorescence quenching spectra of EB–ct-DNA with quinoline hydroperoxide **10b**; dotted line indicates the fluorescence emission spectra of ethidium bromide in absence of ct-DNA and top black line indicates the fluorescence emission spectra of ethidium bromide bound to ct-DNA; $[\text{EB}] = 2 \mu\text{M}$, $[\text{ct-DNA}] = 20 \mu\text{M}$, $[\text{10b}] = 0\text{--}35 \mu\text{M}$ (from top to bottom) with increment of 3.3 μM concentration of **10b**; Arrow indicates the quenching of fluorescence with increasing concentration of quinoline hydroperoxide **10b**; (b) Plot of F_0/F vs [Concentration of **10b**].

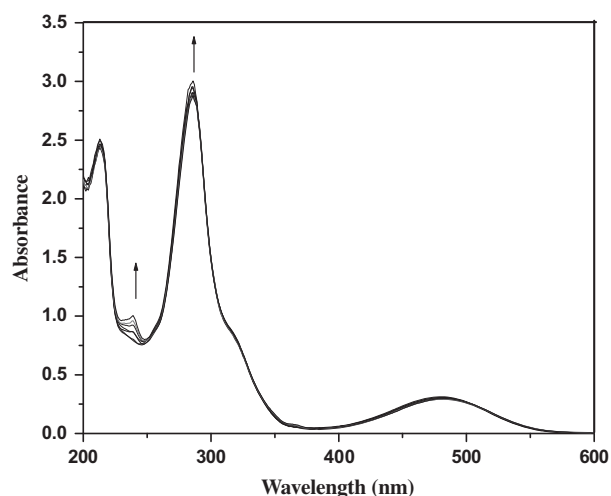


Fig. 10. UV/vis absorption spectra of ethidium bromide (2 μM) in absence (bottom) and presence of quinoline hydroperoxide **10b**, [**10b**] = 0–35 μM (from bottom to top) with increment of 3.3 μM concentration.

hydroperoxide **10b** has an intercalative mode of binding with ct-DNA. (see Fig. 10).

To understand the effect of quinoline hydroperoxide **10b** on ethidium bromide in absence of ct-DNA, we carried out UV/vis absorption study of ethidium bromide with increasing concentration of quinoline hydroperoxide **10b**. With increasing concentration of **10b**, there is slight increase of absorption in 300 nm region due to addition of hydroperoxide **10b**, but in the region of 480 nm there is no change in the absorption, which indicates that quinoline hydroperoxide has no effect on ethidium bromide in absence of ct-DNA.

3.6. Docking study of quinoline hydroperoxide **10b**

Molecular docking study was performed to support the interaction and preferred binding mode of quinoline hydroperoxide **10b** with DNA.

The docking analysis revealed that quinoline hydroperoxide **10b** acts as DNA intercalator. The planar benzoquinoline ring of **10b** intercalated between the base pairs of the DNA helix, while the side chains peroxy group ($-\text{OOH}$) forms weak hydrogen bond

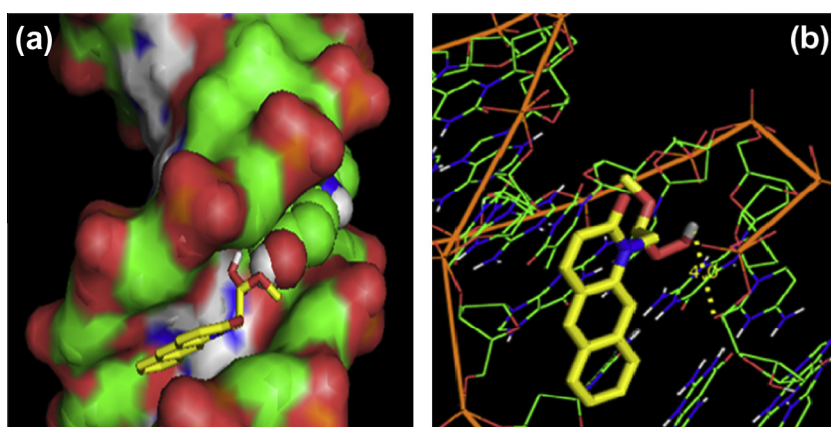


Fig. 11. Docked conformations of quinoline hydroperoxide **10b** with ct-DNA. (a) Surface representation showing the binding pockets of the quinoline hydroperoxide **10b**. (b) Stereoview of the docked conformation of quinoline hydroperoxide **10b** showing the formation of weak H-bonds with cytosine carbonyl.

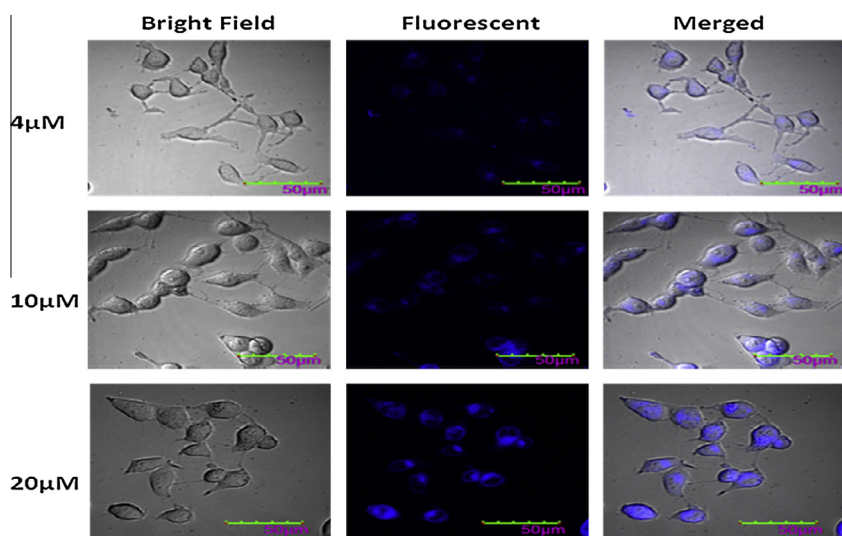


Fig. 12. Confocal micrograph showing intracellular localization of quinoline hydroperoxide **10b** in HeLa cells incubated with the hydroperoxide compound **10b** for 1 h at 37 $^{\circ}\text{C}$. The scale bar corresponds to 50 μm .

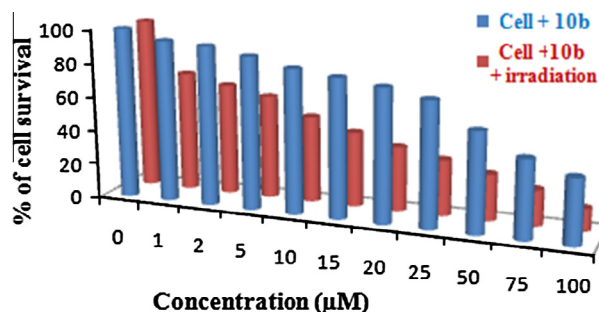


Fig. 13. Cytotoxicity study of quinoline hydroperoxide **10b** in HeLa cells. Data shows the percentage of cell survival of HeLa cells counted after the treatment with hydroperoxide **10b** (0–100 μM) at 37 °C with and without irradiation of UV light for 30 min.

with the carbonyl group of cytosine as reflected in Fig. 11. Thus the docking study corroborates the experimental findings, which suggest that the quinoline hydroperoxide **10b** is behaving as an intercalator of DNA.

3.7. Cell permeability and localization study of quinoline hydroperoxide **10b**

The cell permeability and localization study of quinoline hydroperoxide **10b** was carried out in HeLa cells using confocal fluorescence microscopy. Cells were incubated with different concentrations of quinoline hydroperoxide **10b** (4, 10 and 20 μM) at 37 °C. The confocal images taken after 1 h of incubation, showed dose-dependent rapid internalization and accumulation of the quinoline hydroperoxide **10b** inside the cell (Fig. 12). Significant enhancement in the intracellular fluorescence intensity was observed with increasing concentration of hydroperoxide **10b** from 4–20 μM.

3.8. Cell cytotoxicity studies of quinoline hydroperoxide **10b**

Cell cytotoxicity studies were carried out to evaluate the photocytotoxic effect of quinoline hydroperoxide **10b** using human cervical HeLa cancer cells applying conventional MTT [(3-(4,5-Dimethylthiazol-2-yl)-2,5-diphenyltetrazolium bromide, a yellow tetrazole)] assay (Fig. 13) [46]. Cells were incubated with various concentrations of the quinoline hydroperoxide **10b** (0–100 μM) and cytotoxicity was analyzed in the dark. Further, cells treated with **10b** at different concentrations were irradiated with UV light (≥ 350 nm) for 30 min and cytotoxicity was analyzed in presence of UV light. Cells irradiated with UV light showed moderate decrease in percentage of cell survival giving respective IC_{50} values 9.80 (± 0.65) μM for quinoline hydroperoxide **10b** and the corresponding IC_{50} value analyzed in the dark was 33.32 (± 0.97) μM for **10b**. The MTT assay data showed that the quinoline hydroperoxide **10b** was found to be more cytotoxic upon irradiation of UV light than that of cells which were kept in dark.

4. Conclusion

We have reported the simple, convenient and high yielding synthesis of quinoxaline and quinoline hydroperoxides. The gel electrophoresis data showed concentration dependent DNA cleaving ability of hydroperoxides in presence of UV light (≥ 350 nm). Both singlet oxygen and hydroxyl radicals as reactive oxygen species (ROS) were responsible for the photocleavage of DNA. The quinoline hydroperoxide interacts with DNA via intercalative mode of binding. The confocal fluorescence microscopy of HeLa cells using

the quinoline hydroperoxide reveals localization of the hydroperoxide inside the cell. Further, the quinoline hydroperoxide displayed photocytotoxic effect in HeLa cells giving IC_{50} values in the micromolar range and a dose-dependent photocytotoxicity is observed.

Acknowledgements

We thank DST–SERB for financial support and DST FIST for 400 MHz NMR and Nilanjana Chowdhury is thankful to UGC, New Delhi for fellowship

Appendix A. Supplementary material

Supplementary data associated with this article can be found, in the online version, at <http://dx.doi.org/10.1016/j.jphotobiol.2013.11.010>.

References

- [1] M. Chatterjee, S. Rokita, Sequence-specific alkylation of DNA activated by an enzymatic signal, *J. Am. Chem. Soc.* 113 (1991) 5116–5117.
- [2] I. Saito, M. Takayama, H. Sugiyama, T. Nakamura, In DNA and RNA cleavers and chemotherapy of cancer and viral diseases, in: B. Menunier (Ed.), Kluwer, Netherlands, 1996, pp. 163–176.
- [3] B. Armitage, Photocleavage of nucleic acids, *Chem. Rev.* 98 (1998) 1171–1200.
- [4] L. Perrouault, U. Asseline, C. Rivalle, N.T. Thuong, E. Bisagni, C. Giovannangeli, T. LeDoan, C. Helene, Sequence-specific artificial photo-induced endonucleases based on triple helix-forming oligonucleotides, *Nature* 344 (1990) 358–363.
- [5] W.K. Pogozelski, T.D. Tullius, Oxidative strand scission of nucleic acids: routes initiated by hydrogen abstraction from the sugar moiety, *Chem. Rev.* 98 (1998) 1089–1107.
- [6] I. Saito, M. Takayama, H. Sugiyama, K. Nakatani, A. Tsuchida, M. Yamamoto, Photoinduced DNA cleavage via electron transfer: demonstration that guanine residues located 5' to guanine are the most electron-donating sites, *J. Am. Chem. Soc.* 117 (1995) 6406–6407.
- [7] I. Saito, M. Takayama, S. Kawanishi, Photoactivatable DNA-cleaving amino acids: highly sequence-selective DNA photocleavage by novel L-lysine derivatives, *J. Am. Chem. Soc.* 117 (1995) 5590–5591.
- [8] I. Saito, M. Takayama, T. Sakurai, Photogeneration of carbocation via intramolecular electron transfer: photoinduced DNA alkylation, *J. Am. Chem. Soc.* 116 (1994) 2653–2654.
- [9] I. Saito, M. Takayama, T. Matsuura, Phthalimide hydroperoxides as efficient photochemical hydroxyl radical generators. a novel DNA-cleaving agent, *J. Am. Chem. Soc.* 112 (1990) 884–886.
- [10] S. Matsugo, I. Saito, Photochemical cleavage of *N*-(hydroperoxyalkyl)phthalimides by intramolecular energy transfer, *Tetrahedron Lett.* 25 (1991) 2949–2950.
- [11] I. Saito, Photochemistry of highly organized biomolecules: sequence-selective photoreaction of DNA, *Pure Appl. Chem.* 64 (1992) 1305–1310.
- [12] Y. Xu, X. Qian, W. Yao, P. Mao, J. Cui, Novel naphthalimide hydroperoxide photocleavers: the role of thioacyclic-fused area and the difference in spectra, photochemistry and photobiological activity, *Bioorg. Med. Chem.* 11 (2003) 5423–5427.
- [13] W. Yao, X. Qian, Oxazolonephthalimides and their hydroperoxides: photophysical and photobiological properties, *Dyes Pigms.* 48 (2001) 43–47.
- [14] W. Yao, X. Qian, Synthesis of fluorine-containing oxazolonephthalimide hydroperoxides as DNA photocleavers, *J. Fluorine Chem.* 106 (2000) 69–72.
- [15] W. Yao, X. Qian, Q. Hu, Novel and highly efficient DNA photocleavers: hydroperoxides of heterocyclic-fused naphthalimides, *Tetrahedron Lett.* 41 (2000) 7711–7715.
- [16] H.M. Refaat, A.A. Moneer, O.M. Khalil, Synthesis and antimicrobial activity of certain novel quinoxalines, *Arc. Pharmacol. Res.* 27 (2004) 1093–1098.
- [17] C. Urquiola, M. Vieites, G. Aguirre, Improving anti-trypanosomal activity of 3-aminoquinoxaline-2-carbonitrile N1, N4-dioxide derivatives by complexation with vanadium, *Bioorg. Med. Chem.* 14 (2006) 509–555.
- [18] J. Harmenberg, B. Wahren, J. Bergman, S. Akerfeldt, L. Lundblad, Antiherpetic virus activity and mechanism of action 684 of indolo-(2,3-b)quinoxaline and analogs, *Antimicrob. Agents Chemother.* 32 (685) (1988) 1720–1724.
- [19] B. Zarranz, M. Jaso, L.M. Lima, Antiplasmodial activity of 3-trifluoromethyl-2-carbonylquinoxaline di-N-oxide derivatives, *Rev. Bras. Cienc. Farm.* 42 (2006) 55–67.
- [20] H. Xia, F. Wang, Novel cyclophilin D inhibitors derived from quinoxaline exhibit highly inhibitory activity against rat mitochondrial swelling and Ca²⁺ uptake/release, *Acta Pharmacol. Sin.* 26 (2005) 1201–1211.
- [21] H.J. Chung, O. Jung, Synthesis and biological evaluation of quinoxaline-5,8-diones that inhibit vascular smooth muscle cell proliferation, *Bioorg. Med. Chem. Lett.* 15 (2005) 3380–3384.

- [22] C. Bailly, S. Echebare, F. Gago, Recognition elements that determine affinity and sequence-specific binding to DNA of 2QN, a biosynthetic bis-quinoline analogue of echinomycin, *Anticancer Drug Des.* 15 (1999) 291–303.
- [23] S. Sato, O. Shirator, K. Katagiri, Mode of action of quinoxaline antibiotics: interaction of quinomycin A with deoxyribonucleic acid, *J. Antibiot.* 20 (1967) 270–276.
- [24] H. Cairns, D. Cox, K.J. Gould, A.H. Ingall, J.L. Suschitzky, New antiallergic pyrano[3,2-g]quinoline-2,8-dicarboxylic acids with potential for the topical treatment of asthma, *J. Med. Chem.* 28 (1985) 1832–1842.
- [25] R.J. Steffan, J. Goksoyr, A.K. Bej, R.M. Atlas, Recovery of DNA from soils and sediments, *Appl. Environ. Microbiol.* 54 (1988) 2908–2915.
- [26] F.M. Pohl, T.M. Jovin, W. Baehr, J.J. Holbrook, Ethidium bromide as a cooperative effector of a DNA Structure, *Proc. Nat. Acad. Sci. U.S.A.* 69 (1972) 3805–3809.
- [27] H.M. Berman, J. Westbrook, Z. Feng, G. Gilliland, T.N. Bhat, H. Weissig, I.N. Shindyalov, P.E. Bourne, The protein data bank, *Nucl. Acids Res.* 28 (2000) 235–242.
- [28] G.M. Morris, D.S. Goodsell, R. Huey, A.J. Olson, Distributed automated docking of flexible ligands to proteins: parallel applications of AutoDock 2.4, *J. Comput.-Aided Mol. Des.* 10 (1996) 293–304.
- [29] W.L. DeLano, The PyMOL Molecular Graphics System, DeLano Scientific, San Carlos, CA, USA, 2006 <<http://pymol.sourceforge.net/>>.
- [30] M. Rambaud, M. Bakasse, G. Duguay, J. Villieras, A one-step synthesis of alkyl 2-oxo-3-alkenoates from alkenyl grignard reagents and dialkyl oxalates, *Synthesis* 7 (1988) 564–566.
- [31] S.N. Murthy, B. Madhav, Y.V.D. Nageswar, Revisiting the Hinsberg reaction: facile and expeditious synthesis of 3-substituted quinoxalin-2(1H)-ones under catalyst-free conditions in water, *Helv. Chim. Acta* 93 (2010) 1216–1220.
- [32] A.G. Myers, M.M. Fundy, P.A. Lindstrom Jr., Mild conditions for the acid labile protecting groups, *Tetrahedron Lett.* 29 (1988) 5609–5612.
- [33] J.R. Allen, J.J. Chen, M.J. Frohn, E. Hu, Q. Liu, A.J. Pickrell, S. Rumpf, R.M. Rzas, W. Zhong, Preparation of nitrogen heterocyclic compounds useful as 3',5'-cyclic nucleotide-specific phosphodiesterase 10 (PDE10) inhibitors, *PCT Int. Appl.* 143365 (2011).
- [34] T. Manimaran, T.K. Thiruvengadam, V.T. Ramakrishnan, Synthesis of coumarins (2-oxo-2H-1-benzopyrans), thiocoumarins (2-oxo-2H-1-benzothioopyrans), and carbostyrls (2-oxo-1,2-dihydroquinolines), *Synthesis* 11 (1975) 739–741.
- [35] W.H. Melhuus, Quantum efficiencies of fluorescence of organic substances: effect of solvent and concentration of the fluorescent solute, *J. Phys. Chem.* 65 (1961) 229–235.
- [36] C. Sentagne, B. Meunier, N. Paillous, DNA cleavage photoinduced by new water-soluble zinc porphyrins linked to 9-methoxyellipticine, *J. Photochem. Photobiol. B-Biol.* 16 (1992) 47–59.
- [37] J.R. Hwu, C.C. Lin, C.H. Chuang, K.Y. King, T.R. Su, S.C. Tsay, Aminyl and iminyl radicals from arylhydrazones in the photo-induced DNA cleavage, *Bioorg. Med. Chem.* 12 (2004) 2509–2515.
- [38] M.A.J. Rodgers, P.T. Snowden, Lifetime of oxygen in liquid water as determined by time-resolved infrared luminescence measurements, *J. Am. Chem. Soc.* 104 (1982) 5541–5543.
- [39] A.R. Chakrabarty, Photocleavage of DNA by copper(II) complexes, *J. Chem. Sci.* 118 (2006) 443–453.
- [40] A. Hussain, S. Gadadhar, T.K. Goswami, A.A. Karande, A.R. Chakravarty, Photo-induced DNA cleavage activity and remarkable photocytotoxicity of lanthanide(III) complexes of a polypyridyl ligand, *Dalton Trans.* 41 (2012) 885–887.
- [41] C.Y. Zhou, X.L. Xi, P. Yang, Studies on DNA binding to metal complexes of Saltrien, *Biokhimiya* 72 (2007) 45–51.
- [42] X.J. Dang, M.Y. Nie, J. Tong, H.L. Li, Inclusion of the parent molecules of some drugs with β -cyclodextrin studied by electrochemical and spectrometric methods, *J. Electroanal. Chem.* 448 (1998) 61–67.
- [43] J.F. Li, C. Dong, Study on the interaction of morphine chloride with deoxyribonucleic acid by fluorescence method, *Spectrochim. Acta A* 71 (2009) 1938–1943.
- [44] J.B. Lepecq, C. Paoletti, A fluorescent complex between ethidium bromide and nucleic acids: physical-chemical characterization, *J. Mol. Biol.* 27 (1967) 87–106.
- [45] J.R. Lakowicz, G. Weber, Quenching of fluorescence by oxygen. Probe for structural fluctuations in macromolecules, *Biochemistry* 12 (1973) 4161–4170.
- [46] L.V. Rubinstein, R.H. Shoemaker, K.D. Paul, R.M. Simon, S. Tosini, P. Skehan, D.A. Scudiero, A. Monks, M.R. Boyd, Comparison of in vitro anticancer-drug-screening data generated with a tetrazolium assay versus a protein assay against a diverse panel of human tumor cell line, *J. Natl Cancer Inst.* 82 (1990) 1113–1117.